JOURNAL OF MATERIALS SCIENCE 27 (1992) 580–586

Influence of rapid quenching of the melt on structure and properties of maraging steel

T. A. CHERNYSHOVA, T. V. LYULKINA
Baikov Institute of Metallurgy, USSR Academy of Sciences, Moscow, USSR

Peculiarities of structure, properties and phase transformations in the maraging steel were investigated while quenching from the liquid state. Depending on the solidification rates and subsequent cooling, the formation of highly dispersed structures in the solid phase was possible. The structures were of the following types: fully martensite, fully ferrite; a mixture of ferrite and martensite or martensite and austenite.

1. Introduction

High-alloy maraging steels possessing high strength and technological effectiveness are widely used in modern engineering. Such steels are strengthened by air quenching and ageing at 753–773 K for 1–3 h. The quenched steels have a carbonless martensite structure. During the process of ageing, the supersaturated solid solution disintegrates with precipitation of strengthening phases: Ni_3Ti, NiAl, Ni_3V, Ni_3Mo, Fe_2Mo and others. Increasing the amount of alloying elements leads to the growth in the volume of precipitated phases and to greater dispersion strengthening.

However, a shortage of alloying elements (Ni, Mo, Co, V, etc.) restricts the traditional method of improving the mechanical properties of maraging steels by alloying and predetermines the search for new ways of strengthening steels without decreasing their plasticity and viscosity.

One such way is rapid solidification of the melts, which opens up new opportunities in forming a microcrystalline isotropic structure. The morphological and structural effects due to rapid solidification in iron-based alloys include: (1) a size reduction of dendrite structure (decline in the level of heterogeneity); (2) obtaining supersaturated solid solutions; (3) an increased concentration of point defects; (4) a shift in the temperature ranges of solid-phase transformations; and (5) refining the martensite grain [1, 2].

Distinctive features of rapid solidification and of subsequent phase transformations and their effect on the structure and properties of iron–nickel alloys have been investigated and discussed [1–7]. It was found that the general law of rapid solidification processes is a profound supercooling of the melt prior to the beginning of crystallization, which iron–nickel alloys reaches over 300 K at a cooling rate of 5×10^6–10^7 K s^{-1} and 50–200 K at 5×10^5 K s^{-1} [1]. High supercooling of a melt results in the so-called "mass" (diffusionless) free from segregation crystallization which was observed in most rapidly solidified iron–nickel alloys [1, 3–6, 8]. Reports exist fully diffusionless crystallization leading to the formation of chemically homogeneous grains in the whole volume of a rapidly quenched particle [1, 6]. In most cases, transformation from diffusionless to segregational crystallization was noticed [1, 4–6, 8]. In areas most rapidly cooled, a structure free from segregations is formed. The latent heat released in this process of crystallization causes repeated heating [6]. Therefore, the cooling rate decelerates at the final stage of crystallization, and a few-angled cellular structure with nickel microsegregation is formed. The level of segregation is very small, and the size of the cells is of tenths of a micrometer [4, 9].

Grain refining is one of the advantages of the rapid melt quenching. In iron–nickel alloys produced by conventional solidification the size of an initial austenite grain is about 100 μm, while by a rapid one it is 1–10 μm [7, 10–12].

It is known that the grain size of an initial austenite structure determines that of a martensite formed due to the subsequent phase transformation. Light microscopy methods cannot reveal the martensite structure in rapidly solidified alloys [12]. Electron microscopic examination shows that the size of a martensite plate is less than 1 μm [7]. Such martensite structure refining accounts for a high hardness of martensite iron–nickel alloys. According to published data [9, 11–13] it amounts to 7000 MPa in Fe–(0–15%)Ni alloys and about 9000 MPa in Fe–20% Ni–0.1%C.

In alloys with a higher nickel content, the presence of residual austenite results in a sharp drop of hardness. In fully austenite alloys the hardness reaches 1000 MPa irrespective of their cooling rate. It is noteworthy that in rapidly solidified alloys the austenite is preserved with lower nickel concentrations ($\geqslant 17\%$) than in conventionally quenched alloys ($\geqslant 28\%$) [9]. This is caused by lower M_s in rapidly solidified alloys. In general, M_s is determined by both grain size and alloying element contents in a solid solution. In alloys of similar contents, the higher the cooling rate at crystallization, the lower is the M_s temperature [14].

The investigation of the ageing process of rapidly quenched alloys is of great scientific interest. The volume share of hardening phases is determined by the

0022–2461/92 $03.00 + .12

solubility limit of the alloying elements in the solid state. This limit is low for pure iron and becomes yet lower, when nickel, cobalt and other alloying elements are added. Rapid solidification of the melts provides an essential increase in metal and nonmetal supersaturation levels of iron-based solid solutions.

According to Cantor [6] for most Fe–Me binary alloys, maximum solubility for rapid crystallization is 50%–100% larger than for an equilibrium state.

Wood and Honeycombe [3–5, 8] studied in detail, carbide precipitations in rapidly quenched steel Fe–20 mass % Cr–25 mass % Ni. Their experiments have shown an essential increase in solubility of such elements as Nb, V, Ti, C, B in the investigated steel. Owing to rapid crystallization, they managed to obtain a regular distribution of fine particles of the second phase in the austenite matrix, to prevent carbide $Me_{23}C_6$ formation on the grain boundaries, and to obtain selective formation of more stable and coarse-resistant strengthening phases due to special alloying (Nb, V).

This paper describes the results of an investigation aimed at demonstrating what anomalies may occur while rapidly quenching maraging steels, and at analysing potential possibilities of this method for increasing the strength properties of steels of this class.

The object of this investigation is maraging steel containing 17% Ni, 12% Co, 5% Mo and 1.3% Ti. This alloy is of great interest not only due to the effects achieved earlier on the rapidly quenched binary Fe–Ni alloys, but also due to its ability to harden in supersaturated solid solution ageing.

2. Experimental procedure

The maraging steel containing 0.006% C, 17.5% Ni, 12.4% Co, 4.94% Ho, 1.35% Ti was melted to a pure mixture in a vacuum arc furnace under an excessive argon pressure. Its rapid quenching was conducted by: (1) dispersion of the melt by means of a high-temperature gas flow with subsequent cooling on a rapidly rotating copper roller; (2) two-piston quenching; (3) melt spinning in a helium atmosphere.

The morphology and microstructure of rapidly solidified particles were studied by light, scanning and transmission electron microscopy ("Neofot-2", JSM-V3 and JEM 200A microscopes were used). An electrolite of 5% perchloric acid/95% glacial acetic acid, a voltage of 40 V, and a temperature of 273 K were used to prepare thin foils for transmission electron microscopy.

The temperature ranges of phase transformations were measured by differential thermal analysis. Microhardness testing and X-ray diffractometry (XRD) were used. Cooling rates during solidification were estimated using a dendritic parameter.

The conventional ingot microstructure of the investigated steel is a b c c martensite. Its microhardness is 3500 MPa. Differential thermal analysis (DTA) indicates the M_s temperature to be 573 K.

3. Results and discussion

Scanning electron microscopy shows that the shape of rapidly quenched particles obtained according to the first scheme changes from scaly to spherical. The scales were formed by flattening the melt drops against the rapidly rotating copper roller and were probably crystallized when coming into contact with it, at a high cooling rate of $\sim 10^7\ K\,s^{-1}$ (Fig. 1a, b). The thickness of the scales varied within 6–10 μm. The cooling rate increased according to the size reduction of the scales.

Spherical particles were formed due to crystallization of the melt drops without contacting the roller, and thus, were less intensively cooled. The cooling rate during solidification was 10^3–$10^4\ K\,s^{-1}$. Usually the diameter of spherical particles was less than 50 μm.

Table I shows the XRD results and the microhardness of rapidly quenched scales. The structure of the rapidly quenched particles consists of b c c and f c c components which testifies to the stabilization of the austenite and the decrease in M_s temperature. Different combinations of structural components determine the variation in scale microhardness, from 4000–6000 MPa.

The results of chemical analysis and X-ray diffraction show the presence of the oxide Fe_3O_4 in the rapidly quenched scales, its amount increasing sharply as the size of the scales decreases.

As is known, oxides severely deteriorate the quality of a powder and its subsequent compacting. Two-piston quenching has no such drawback, because the melt is quenched in vacuum. By crystallizing the melt drops between copper pistons, foils 15–30 mm diameter and 50–100 μm thick were formed. The cooling rate reaches 10^5–$10^6\ K\,s^{-1}$. The phase composition of the foils is represented by only a martensite b c c phase ($a = 0.28739$ nm). According to DTA, the temperature of the starting point of martensite transformation dropped to 473 K. Transmission electron microscopy shows (Fig. 1d) that the width of the martensite plates in the foils is 0.3–0.4 μm. The microhardness values vary from 5000–6000 MPa to 8000–10000 MPa with different foils.

The structure and properties of ribbons produced by melt spinning depend on the roller rate, V_r (Table II). When V_r is $20.9\ m\,s^{-1}$, a ferrite structure component appears in the maraging steel, and when V_r is $27.7\ m\,s^{-1}$ a completely ferrite structure is formed (Fig. 1e, f, g). A 1.5–2 μm ferrite grain was found metallographically in these ribbons.

Ferrite formation is an anomaly for the investigated maraging steel. This b c c phase was identified as α-ferrite, because it has no metallographical signs of martensite, and its hardness is 700–1000 MPa, less than that of the conventional ingot. Further increase of roller speed leads to a decrease in the ferrite components share. When V_r reaches $41.6\ m\,s^{-1}$, martensite structure is formed completely (Fig. 1h). In this case the size of the martensite packets is 2 μm in comparison with 100 μm in the conventional ingot. Such a high fineness of the structure explains the great increase in hardness of the martensite produced by rapid quenching.

The feasibility of obtaining various microstructures by varying the cooling rate during the process of

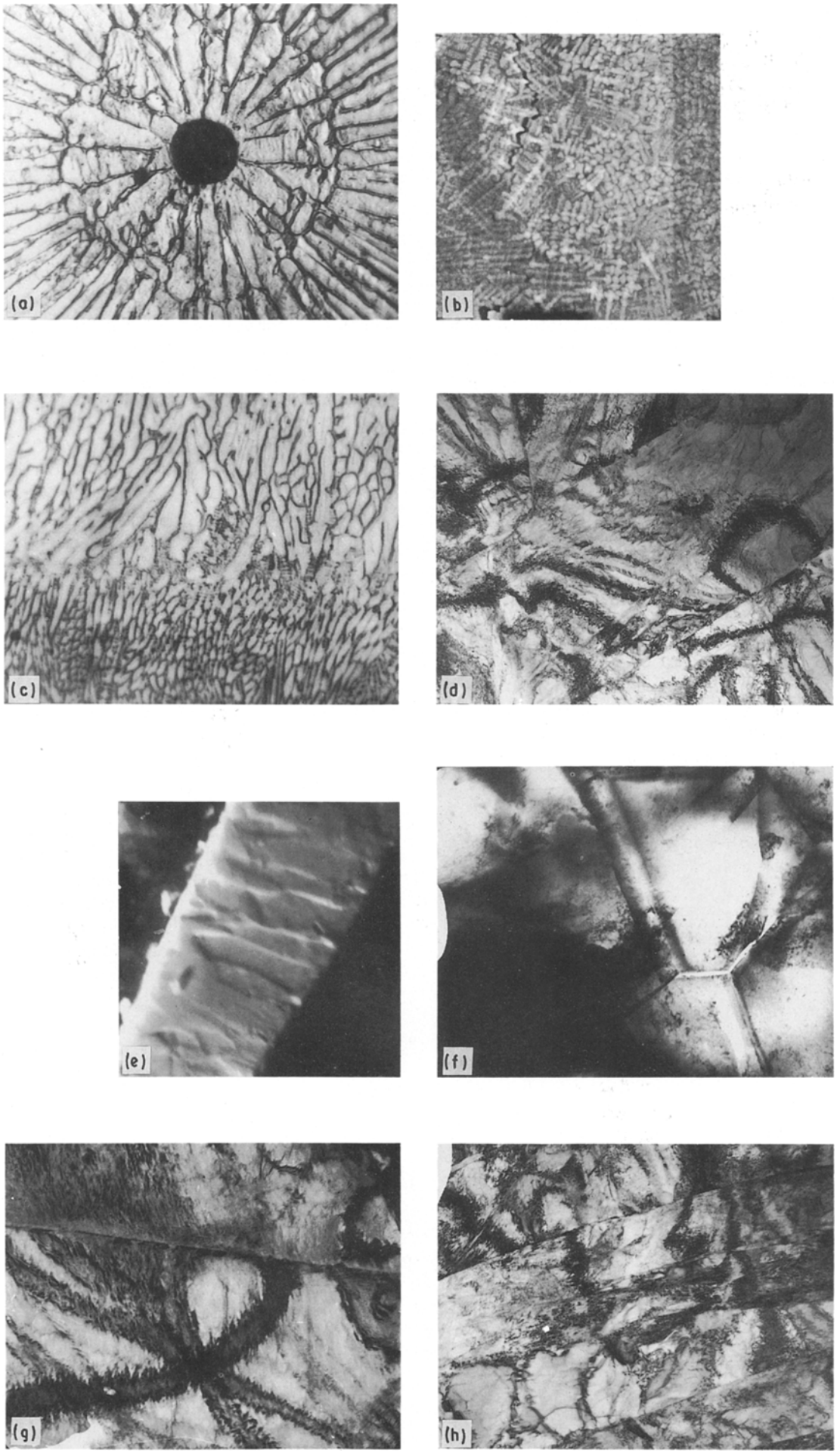

Figure 1 Structure of rapidly quenched steel. (a, b) Plasma dispersion; (c, d) two-piston quenching; (e–g) melt spinning at cooling surface rate $V_r = 27.7\,m\,s^{-1}$; (h) the same at $V_r = 41.6\,m\,s^{-1}$; (a, c, e, h) ×2500; (b, d, f) ×15000; (g) $NiTi_2$ precipitation in ferrite, ×28000.

TABLE I The phase relationship and microhardness of rapidly quenched scales

Scale size (μm)	Phase composition	b c c (f c c) lattice parameter (nm)	Microhardness (MPa)
200	b c c + 6% f c c	0.28700 (0.35869)	4200
200–160	b c c + 10% f c c + trace of Fe_3O_4	0.28706 (0.35929)	6000
160–100	b c c + 16% f c c + trace of Fe_3O_4	0.28714 (0.35929)	4000
100–63	b c c + 26% f c c + 8% Fe_3O_4	0.28727 (0.35961)	4200
63–50	b c c + 32% f c c + 10% Fe_3O_4	0.28727 (0.35961)	4500

TABLE II Structure and properties of melt-spun maraging steel

V_r ($m\,s^{-1}$)	Ribbon width (mm)	Ribbon thickness (μm)	Cooling rate ($K\,s^{-1}$)	Phase composition	b c c lattice parameter (nm)	Microhardness (MPa)
20.9	4.7 ± 1.2	45 ± 5	4×10^6	F + 25% M		3389 ± 137
27.7	4.0 ± 0.8	33 ± 3	6.5×10^6	F	0.28703	2789 ± 98
34.8	3.5 ± 0.6	27 ± 4	9.2×10^6	M + 20% F		3502 ± 118
41.6	3.2 ± 0.7	23 ± 2	1.2×10^7	M	0.28740	5206 ± 147

F-ferrite, M-martensite.

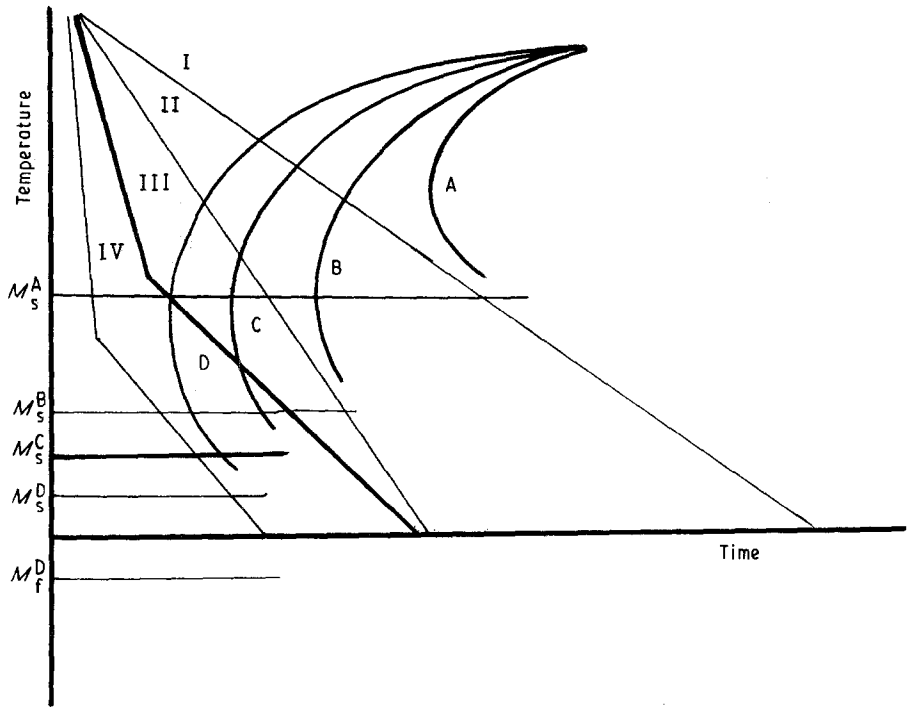

Figure 2 Schematic representation of f c c → b c c transformation in the maraging steel with changes in conditions of crystallization and cooling: A, I, the ingot; B, II, two-piston quenching of the melt; C, III, melt spinning; D, IV, plasma dispersion of the melt.

solidification and subsequent cooling in the solid state, has already been discussed by Cantor [6] and may be represented as shown in Fig. 2. The position of the f c c → b c c diffusion transformation curves (A–D) and the temperature ranges of the martensite transformation are determined by the austenite grain size. The temperature–time curves, describing melt spinning and plasma dispersion regimes, have a characteristic bend corresponding to breaking the contact between the cooling surface and the crystallized particle (ribbon or scales), and this leads to a sharp drop in cooling rate. If such a break of contact takes place at sufficiently high temperature (III), the diffusional transformations can be realized.

This fact was confirmed by transmission electron microscopy data: in the structure of ferrite grains, $NiTi_2$ precipitates were discovered (Fig. 1g). Apparently these were precipitated in the melt-spinning regime during the slow cooling stage of the ferrite solid solution.

When the maraging steel was dispersed in a high-temperature gas flow and cooled on a rapidly rotating copper roller, thinner scales were obtained. The temperature at which they break contact with the roller

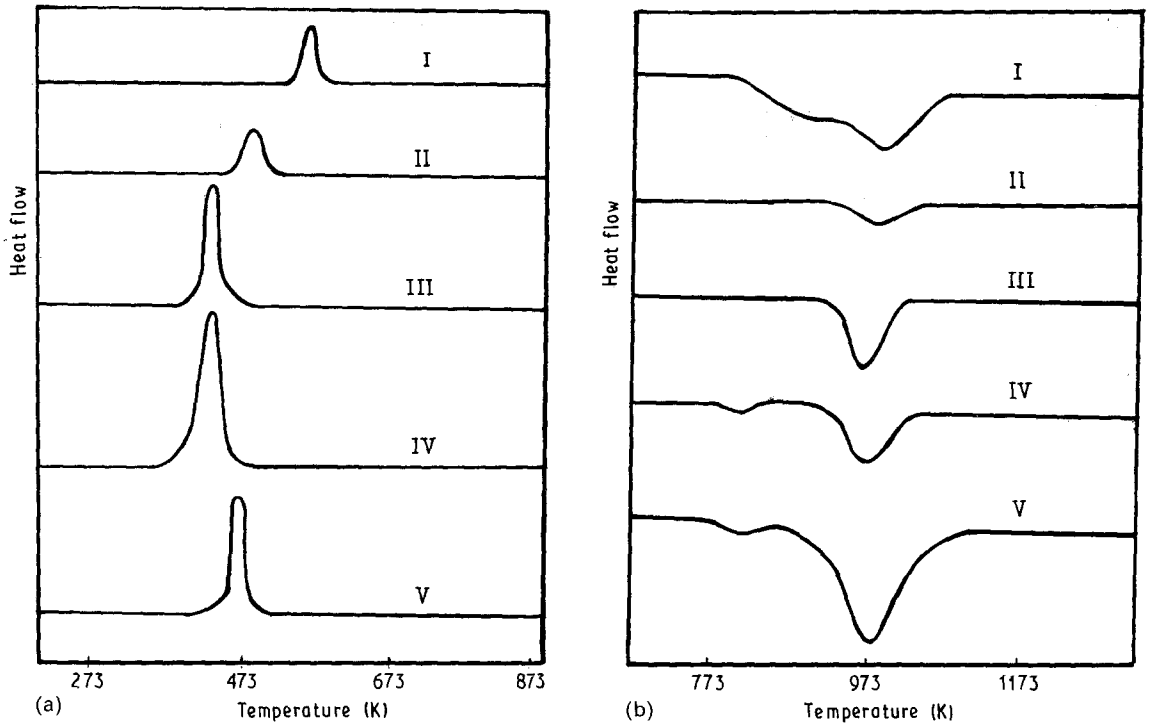

Figure 3 DTA curves of the maraging steel. (a) Exotherms of transformation while cooling; (b) endotherms of transformation while heating. I, the ingot; II, the foil obtained with two-piston quenching; III, the ribbon obtained by spinning at $V_r = 20.9\ m\,s^{-1}$; IV, V, the same after 1223 K annealing for 30 and 60 min, respectively.

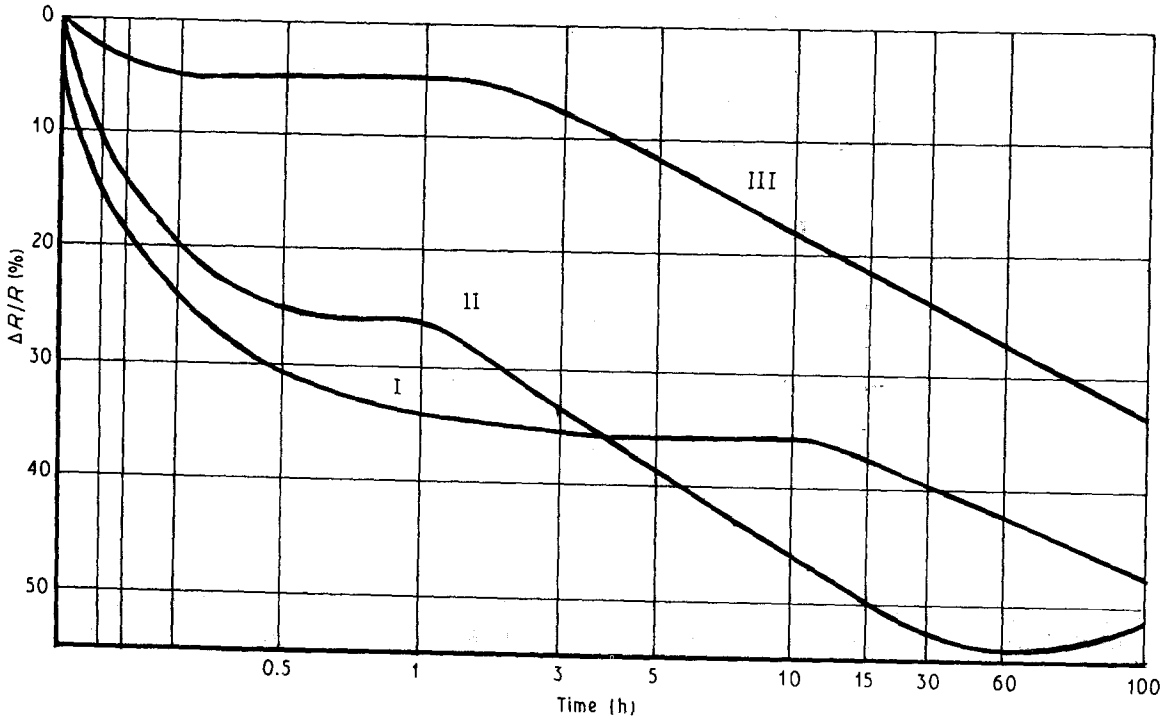

Figure 4 Change in electrical resistance of steel on heating rapidly quenched martensite (I), ingot martensite (II), and rapidly quenched ferrite (III).

surface is lower. Therefore, f c c → b c c transformation has a martensite mechanism, extremely fine-crystalline two-phase martensite + austenite structure being formed.

In the process of melt spinning, regulation of the phase relationship can be realized. The reduction of stability of fine-grained supercooled austenite, on the one hand, and the various ribbon temperatures at the point of breaking contact with the roller, on the other, lead to the formation of a ferrite and martensite mixture when the roller speed is 20.9 or 34.8 $m\,s^{-1}$. Increasing the roller speed up to 41 $m\,s^{-1}$ leads to such a decrease in temperature for a thinner ribbon at the point of breaking contact with the cooling surface, that the $\gamma \rightarrow \alpha$ transformation occurs by the martensite mechanism.

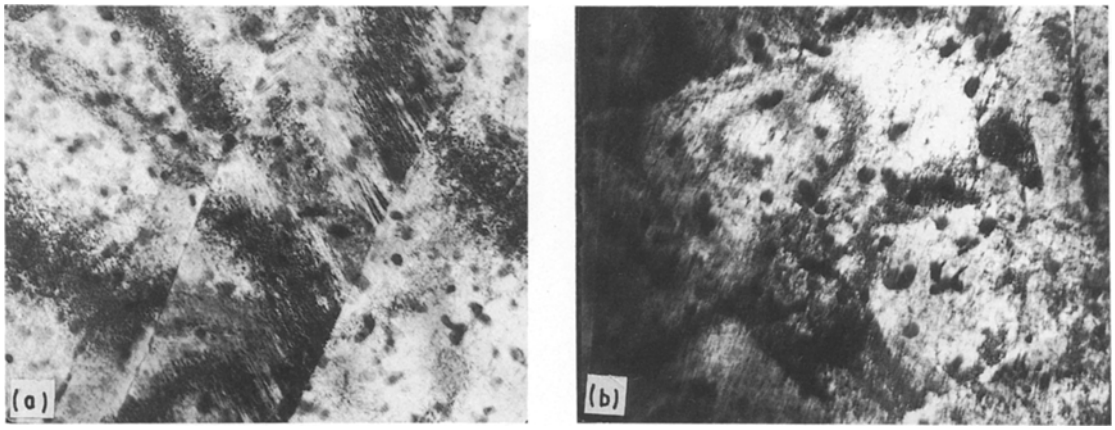

Figure 5 Structure of rapidly quenched steel after ageing (773 K, 3 h): (a) martensite, × 25 000; (b) ferrite, × 15 000.

The proposed schemes are confirmed by the DTA data: the M_s temperature of rapidly quenched particles was 80–120 K lower compared with the conventional ingot (Fig. 3).

On repeatedly heating these particles up to bcc → fcc transformation temperature, the melt rapid-quenching effect relaxation occurs, the martensite transformation temperature increasing gradually up to M_s of the conventional ingot.

One of the main advantages of melt quenching is the small grain size. The methods of melt quenching used in the present investigation allow us to obtain martensite structure with a martensite plate width of 0.3–0.4 μm and packet dimensions of 2–5 μm, compared with 100 μm in the ingot; the ferrite structure has a grain size of 1.5–2 μm. The increase in hardness of rapidly quenched martensite proves that the interface boundary is a decisive factor in alloy strengthening.

It is well-known that the maraging steels have a stronger age-hardening response. The strength and the hardness of melt-spun ribbons ($V_r = 41.6\,m\,s^{-1}$) after ageing (773 K, 3 h) are 3500 and 8600 MPa, respectively. These values are 2300 and 5580 MPa in maraging steel produced by traditional technology.

The electrical resistance method has shown an increase in ageing rate during the early stage of the precipitation process, and a slower coarsening of the precipitates in rapidly quenched martensite, compared with conventional martensite (Fig. 4).

Phases precipitated during rapidly quenched and conventional martensite ageing have the same crystallographic nature: hcp Ni_3Ti phase (Fig. 5). The increase in hardness is 3400 and 2350 MPa due to ageing in the rapidly quenched and conventional martensite, respectively. The precipitation hardening of ferrite differs from martensite ageing both in the process kinetics and crystallographic nature of the precipitating phases. Transmission electron microscopy showed that the ferrite hardening was caused by the cubic $NiTi_2$ phase precipitates. This phase had already been precipitated from the solid solution during melt spinning. Further heating results in a coarsening of these precipitates. The hardness increase as a result of ageing of the rapidly quenched ferrite, is only 660 MPa.

4. Conclusions

1. Rapid quenching of maraging steel melts affects significantly the character of phase transformations, structure and properties of steels. The experiments have shown the feasibility of forming structures of the following types: (1) all martensite; (2) all ferrite; (3) a mixture of martensite and austenite or martensite and ferrite components, depending on the cooling rate during solidification and subsequent cooling.

2. The microcrystalline structure of the initial austenite formed by rapid quenching of maraging steel enables fine crystalline products to be obtained in the subsequent solid-phase transformations. They are: ferrite with grain diameter 1.5–2 μm, martensite with a packet size 2–5 μm, and plate width 0.3–0.4 μm. Maximum values of microhardness (5000–7000 MPa) were obtained when a fine-crystalline martensite structure had been formed in the rapidly quenched steel.

3. The age hardening of rapidly quenched steel results from precipitation of the Ni_3Ti phase from a martensite solid solution, and of the $NiTi_2$ phase from ferrite solid solution, the aged hardness of rapidly quenched martensite (in melt-spun ribbons) increasing to 8600 MPa. Owing to essential supersaturation of the solid solution and peculiarities of ageing kinetics, the hardness increase in rapidly quenched martensite steel is almost twice that of the conventional one.

References

1. C. HAYZELDEN, J. J. RAYMENT and B. CANTOR, *Acta Metall.* **31** (1983) 379.
2. J. V. WOOD and C. GAGG, in "Rapidly Solidified Metastable Materials" Boston, MA, 14–17 November 1983 (1984) pp. 151–5.
3. J. V. WOOD and R. W. K. HONEYCOMBE, *Phil. Mag. A* **37** (1978) 501.
4. *Idem.*, Mater. Sci. Engng **23** (1976) 107.
5. *Idem., ibid.* **38** (1979) 217.
6. B. CANTOR, in "Rapidly solidified amorphous and crystalline alloys", edited by B. H. Kear, B. C. Giessen and M. Cohen (Elsevier Science, North Holland, NY, 1982) pp. 317–30.

7. Y. INOKUTI and B. CANTOR, *Acta Metall.* **30** (1982) 343.
8. J. V. WOOD and R. W. K. HONEYCOMBE, *J. Mater. Sci.* **9** (1974) 1183.
9. F. DUFLOS and B. CANTOR, in "Rapidly quenched metals", edited by B. Cantor (Metallurgia, Moscow, 1983) pp. 81–8.
10. Y. LHANG, F. DUBKOVSKY, S. KANGAND and N. J. GRANT, *Powder Metall. Int.* **1** (1985) 17.
11. Y. INOKUTI and B. CANTOR, *Scripta Metall.* **10** (1976) 655.
12. *Idem., J. Mater. Sci.* **12** (1977) 946.
13. C. HAYZELDEN and B. CANTOR, *Int. J. Rapid. Solid.* **1** (1985) 237.
14. *Idem.*, in "Solid–Solid Phase Transformations", edited by H. I. Aaronson, D. E. Laughlin, R. F. Sekera and C. M. Wayman (AIME, 1983) pp. 1397–1401.

Received 18 December 1989
and accepted 1 May 1991